

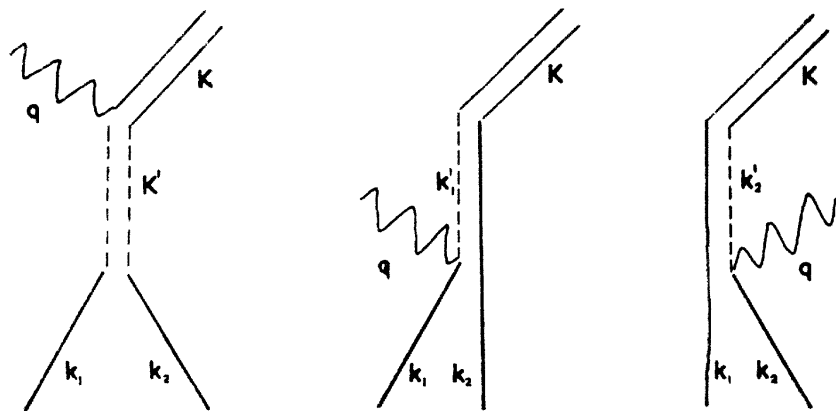
Overview on coalescence model: Theoretical developments and applications

Che-Ming Ko
Texas A&M University

Workshop on Exotic Hadrons from High Energy Collisions,
Kyoto, Japan, March 23 -26, 2016

The coalescence model

- 1960s
 - 1) Butler and Pearson, PR 129, 836 (1963): Two nucleons coalesce into a deuteron with the nuclear matter acting as a catalyst. In second-order perturbation theory,



$$N_d(\mathbf{K}) \propto [N_p(\mathbf{K}/2)]^2$$

- 2) Schwalzschild and Zupancic, PR 129, 854 (1963): The deuteron-to-proton ratio is governed by the probability of finding a neutron within a small sphere of radius ρ around the proton in momentum space

$$dN_d(\mathbf{K})/dN_p(\mathbf{K}/2) \propto \frac{4\pi\rho^3}{3}$$

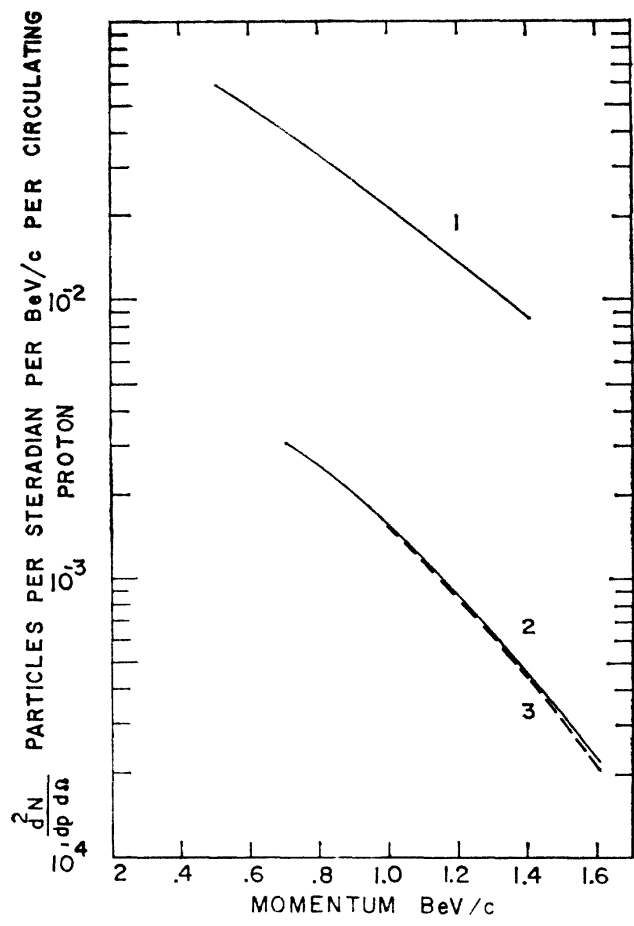


FIG. 3. A comparison of the observed and calculated momentum distributions for deuterons produced from a Be target at an angle of 45° in the laboratory system by protons with incident energy 30 BeV. Curves 2 and 3 are the observed and the calculated deuteron distribution (34). Curve 1 is the experimental distribution of cascade protons used to calculate (34). The experimental data are those of Fitch *et al.* (reference 3).

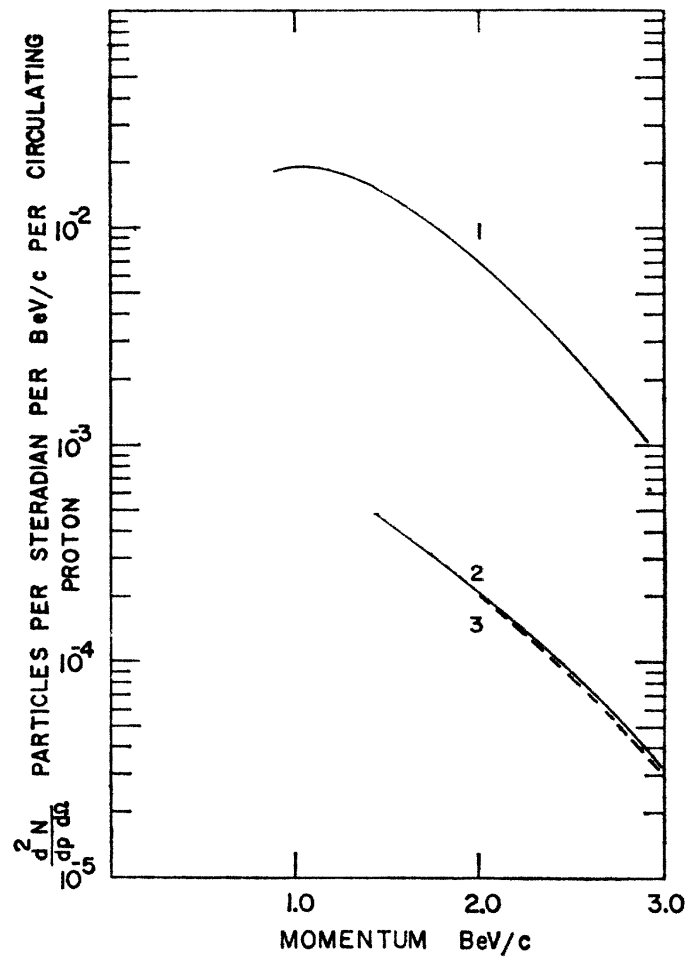


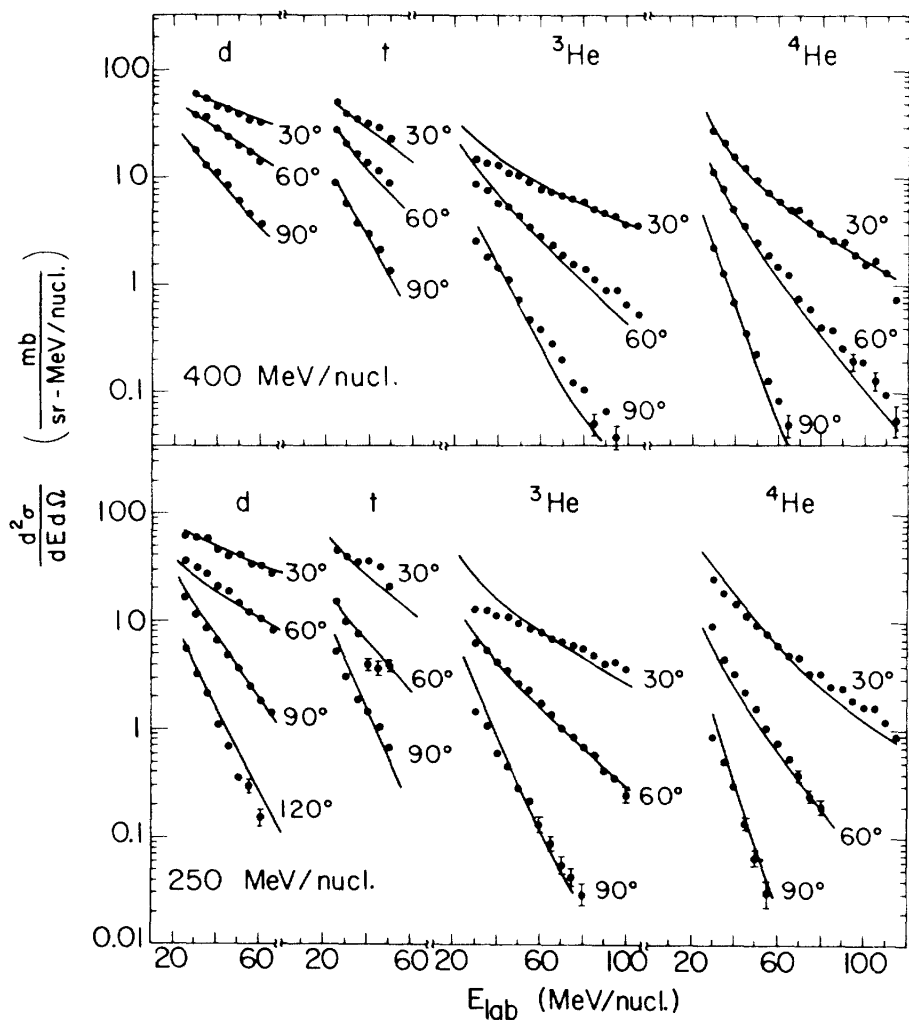
FIG. 4. As in Fig. 3, the deuterons are produced from a Be target at an angle of 30° in the laboratory system by protons with incident energy 30 BeV. The curves are labeled as in Fig. 3, and the experimental results are those of Schwarzschild and Zupančič (reference 6).

- 1970s
 - 1) Gutbrod et al., PRL 37, 667 (1976): Momentum spectra of light nuclei in HIC are related to that of nucleons, with the coalescence parameter B_A related to the coalescence radius p_0 in momentum space

$$E_A \frac{d^3 N_A}{dp_A^3} = B_A \left(E_p \frac{d^3 N_p}{dp_p^3} \right)^A, \quad p_A = A p_p$$

$$B_A = \left(\frac{4\pi}{3} p_0^3 \right)^{A-1} \frac{M}{m^A}$$

- 2) Das and Hwa, PLB 68, 459 (1977): Quark recombination for hadron production in fragmentation region of pp collisions.
- 3) Bond, Johanson, Koonin, and Garpman, PLB 71, 43 (1977): Coalescence is formulated in the sudden approximation
- 4) Mekjian, PRC 17, 1901 (1978): Kinetic approach to light nuclei production, e.g., $n+p+N \leftrightarrow d+N$ like in nucleosynthesis in stars.



Gutbrod et al., PRL 37, 667 (1976)

Coalescence radius
 p_0 (MeV)

Nuclei	250	400
d	126	129
t	140	129
^3He	135	129
^4He	157	142

FIG. 3. Experimental points and calculated lines for the double-differential cross sections of fragments from the irradiation of uranium by ^{20}Ne ions at 250 and 400 MeV/nucleon.

Coalescence model in the sudden approximation

Wave functions for
initial $|i\rangle = |1,2\rangle$
and final $|f\rangle = |3\rangle$
states

Probability for $1+2 \rightarrow 3$ $\mathcal{P} = |\langle f|i \rangle|^2$

Probability for particle 1 of momentum \mathbf{k}_1 and particle 2 of momentum \mathbf{k}_2 to coalescence to cluster 3 with momentum \mathbf{K}

$$\frac{dN}{d^3\mathbf{K}} = g \int d^3\mathbf{x}_1 d^3\mathbf{k}_1 d^3\mathbf{x}_2 d^3\mathbf{k}_2 W_1(\mathbf{x}_1, \mathbf{k}_1) W_2(\mathbf{x}_2, \mathbf{k}_2) \\ \times W(\mathbf{y}, \mathbf{k}) \delta^{(3)}(\mathbf{K} - \mathbf{k}_1 - \mathbf{k}_2), \quad \mathbf{y} = \mathbf{x}_1 - \mathbf{x}_2, \quad \mathbf{k} = \frac{\mathbf{k}_1 - \mathbf{k}_2}{2}$$

Wigner functions $W(\mathbf{x}, \mathbf{k}) = \int d^3\mathbf{y} \phi^* \left(\mathbf{x} - \frac{\mathbf{y}}{2} \right) \phi \left(\mathbf{x} + \frac{\mathbf{y}}{2} \right) e^{-i\mathbf{k}\cdot\mathbf{y}}$

For a system of particles 1 and 2 with phase-space distributions $f_i(\mathbf{x}_i, \mathbf{k}_i)$ normalized to $\int d^3\mathbf{x}_i d^3\mathbf{k}_i f_i(\mathbf{x}_i, \mathbf{k}_i) = N_i$, number of particle 3 produced from coalescence of N_1 of particle 1 and N_2 of particle 2

$$\begin{aligned} \frac{dN}{d^3\mathbf{K}} &= g \int d^3\mathbf{x}_1 d^3\mathbf{k}_1 d^3\mathbf{x}_2 d^3\mathbf{k}_2 f_1(\mathbf{x}_1, \mathbf{k}_1) f_2(\mathbf{x}_2, \mathbf{k}_2) \\ &\times \overline{W}(\mathbf{y}, \mathbf{k}) \delta^{(3)}(\mathbf{K} - \mathbf{k}_1 - \mathbf{k}_2) \end{aligned}$$

$$\overline{W}(\mathbf{y}, \mathbf{k}) = \int \frac{d^3\mathbf{x}'_1 d^3\mathbf{k}'_1}{(2\pi)^3} \frac{d^3\mathbf{x}'_2 d^3\mathbf{k}'_2}{(2\pi)^3} W_1(\mathbf{x}'_1, \mathbf{k}'_1) W_2(\mathbf{x}'_2, \mathbf{k}'_2) W(\mathbf{y}', \mathbf{k}')$$

Wigner function $W_i(\mathbf{x}'_i, \mathbf{k}'_i)$ centers around \mathbf{x}_i and \mathbf{k}_i

$$g = \frac{2J+1}{(2J_1+1)(2J_2+1)} \quad \text{Statistical factor for two particles of spin } J_1 \text{ and } J_2 \text{ to form a particle of spin } J$$

The above formula can be straightforwardly generalized to multi-particle coalescence.

- 1980s
 - 1) Kapusta, PRC 21, 1301 (1980): Comparison of coalescence model, sudden approximation, and thermal model for deuteron production.
 - 2) Sato and Yazaki, PLB 98, 153 (1981): Density matrix formalism for evaluating the coalescence parameter.

Deuteron : $\frac{4\pi}{3}p_0^3 = \frac{3}{4} \cdot 2^{3/2}(4\pi)^{3/2}[\nu_d\nu/(\nu_d + \nu)]^{3/2}$

Triton : $\frac{1}{2} \left(\frac{4\pi}{3}p_0^3 \right)^2 = \frac{1}{4} \cdot 2^{3/2}(4\pi)^3[\nu_t\nu/(\nu_t + \nu)]^3$

Alpha : $\frac{1}{4} \left(\frac{4\pi}{3}p_0^3 \right)^3 = \frac{1}{16} \cdot 2^{3/2}(4\pi)^{9/2}[\nu_\alpha\nu/(\nu_\alpha + \nu)]^{9/2}$

ν and ν_A are size parameters of emitting source and nuclei, respectively

→ B_A decreases with source size ($1/\nu$) and size ($1/\nu_A$) of nuclei

- 1980s
- 3) Gyulassy, Frankel, and Remler, NPA 402, 596 (1983): Generalized coalescence model using nucleon Wigner functions that are delta functions in space and momentum, i.e., evaluating

$$\overline{W}(\mathbf{y}, \mathbf{k}) = \int \frac{d^3\mathbf{x}'_1 d^3\mathbf{k}'_1}{(2\pi)^3} \frac{d^3\mathbf{x}'_2 d^3\mathbf{k}'_2}{(2\pi)^3} W_1(\mathbf{x}'_1, \mathbf{k}'_1) W_2(\mathbf{x}'_2, \mathbf{k}'_2) W(\mathbf{y}', \mathbf{k}')$$

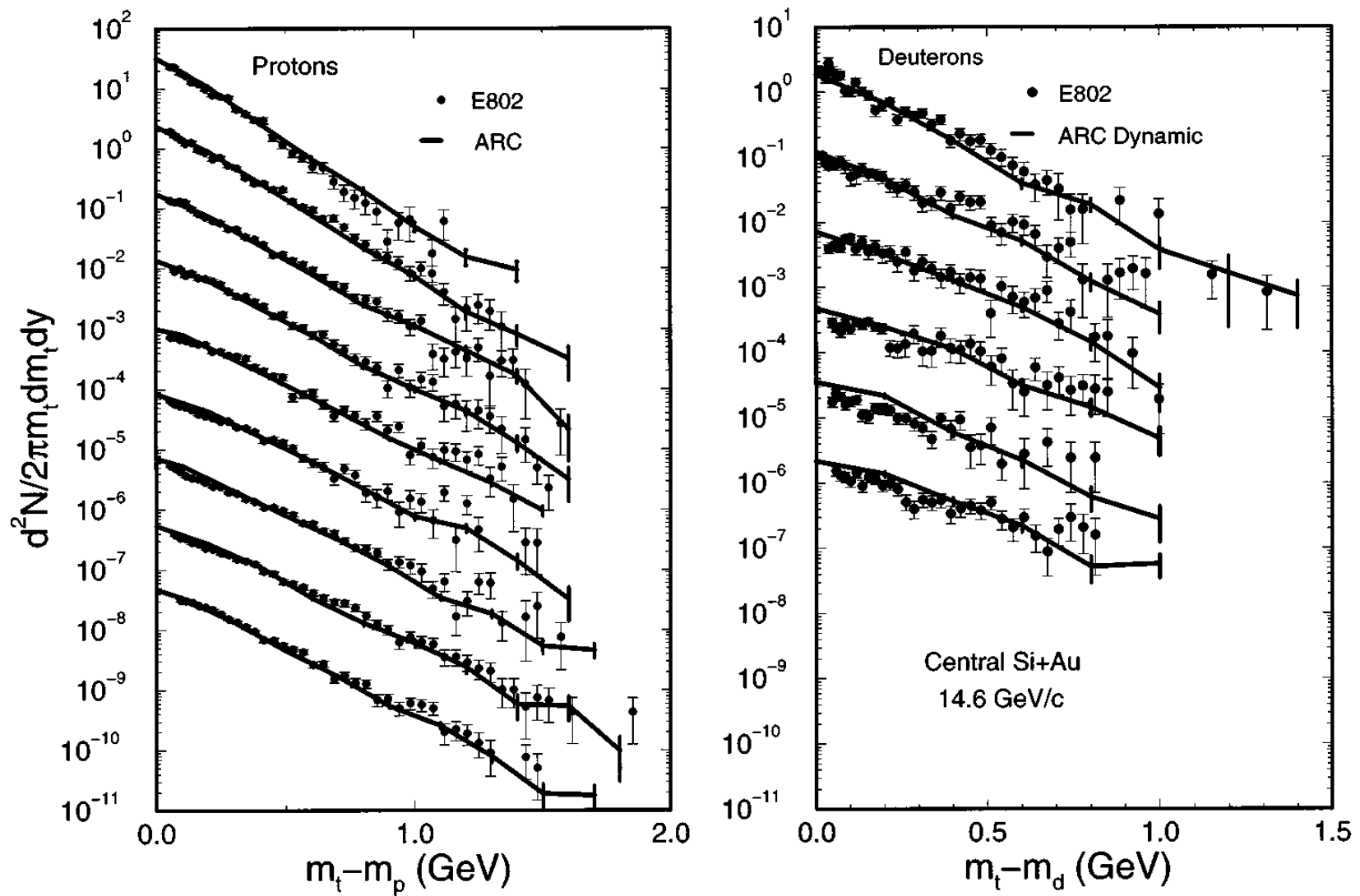
with $W_i(\mathbf{x}'_i, \mathbf{k}'_i) = (2\pi)^3 \delta^3(\mathbf{x}'_i - \mathbf{x}_i) \delta^3(\mathbf{k}'_i - \mathbf{k}_i)$

$$\begin{aligned} \rightarrow \frac{dN}{d^3\mathbf{K}} &\approx g \int d^3\mathbf{x}_1 d^3\mathbf{k}_1 d^3\mathbf{x}_2 d^3\mathbf{k}_2 f_1(\mathbf{x}_1, \mathbf{k}_1) f_2(\mathbf{x}_2, \mathbf{k}_2) \\ &\times W(\mathbf{y}, \mathbf{k}) \delta^{(3)}(\mathbf{K} - \mathbf{k}_1 - \mathbf{k}_2) \end{aligned}$$

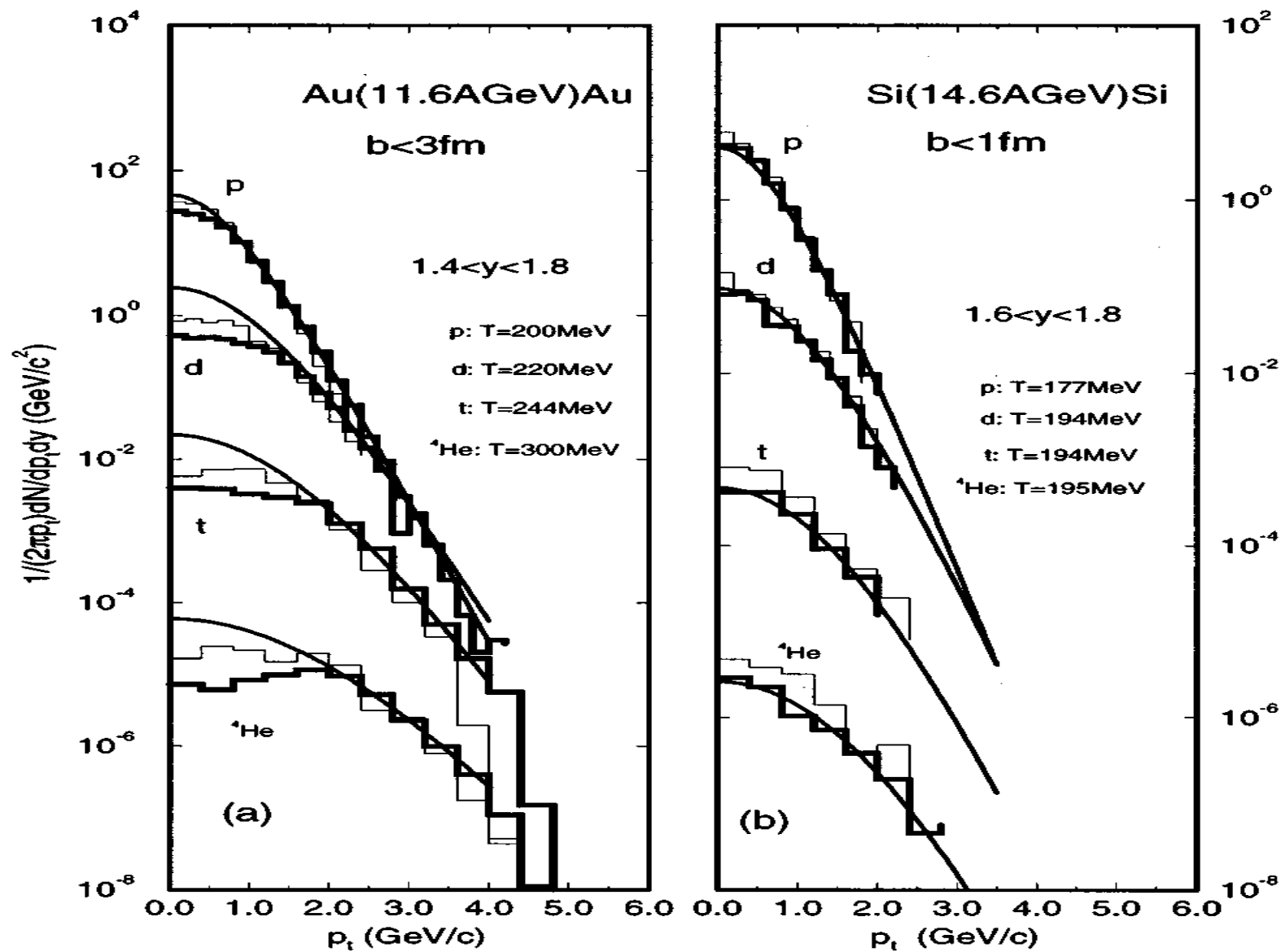
It is later called by Khahana et al. the standard Wigner calculation in contrast to the general one which they called the quantum Wigner calculation.

- 1990s
 - 1) Danielewicz and Bertsch, NPA 533, 712 (1991):
Deuteron production in transport model including $p+n+N \leftrightarrow d+N$.
 - 2) Dover, Heinz, Schneidermann, and Zimanyi, PRC 44, 1636 (1991):
Covariant coalescence model for d , $d\bar{n}$, and H dibaryon.
 - 3) Mrowczinski, PLB 277, 43 (1992): Similarity between
proton-neutron correlations and deuteron production.
 - 4) Baltz et al., PLB 325, 7 (1994): Simplified coalescence model,
 $dr < (dr)_{\max}$, $dp < (dp)_{\max}$.
 - 5) Kahana et al., PRC 54, 388 (1996): Quantum Wigner calculation
based on A Relativistic Cascade (ARC) model.
 - 6) Baltz and Dover, PRC 53, 362 (1996): p-wave Wigner function for
 $K+K\bar{b}ar \rightarrow \phi$.
 - 7) Mattiello, Sorge, Stocker, and Greiner, PRC 55, 1443 (1997): Light
nuclei production based on standard Wigner calculation using
nucleon phase-space distributions from RQMD.

Kahana et al., PRC 54, 388 (1996)



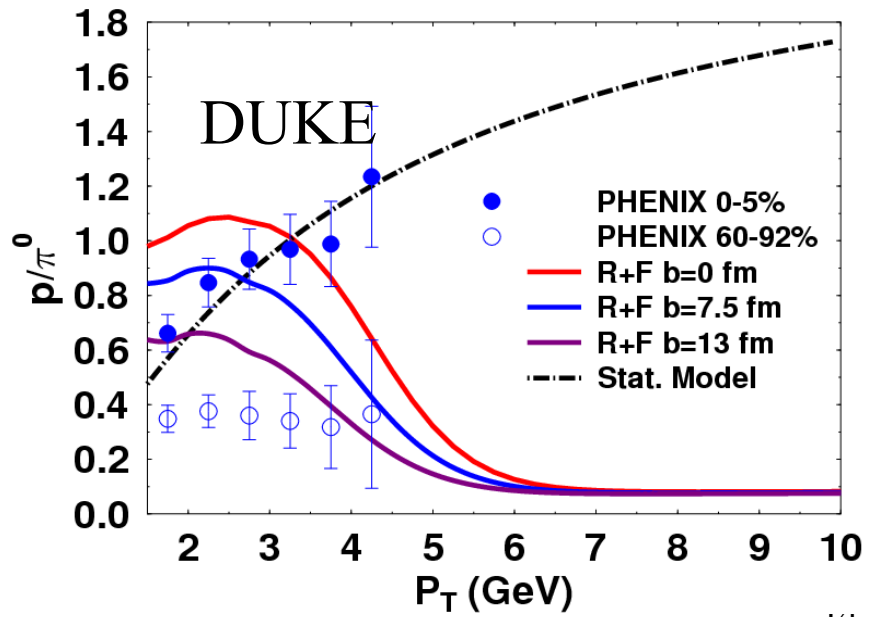
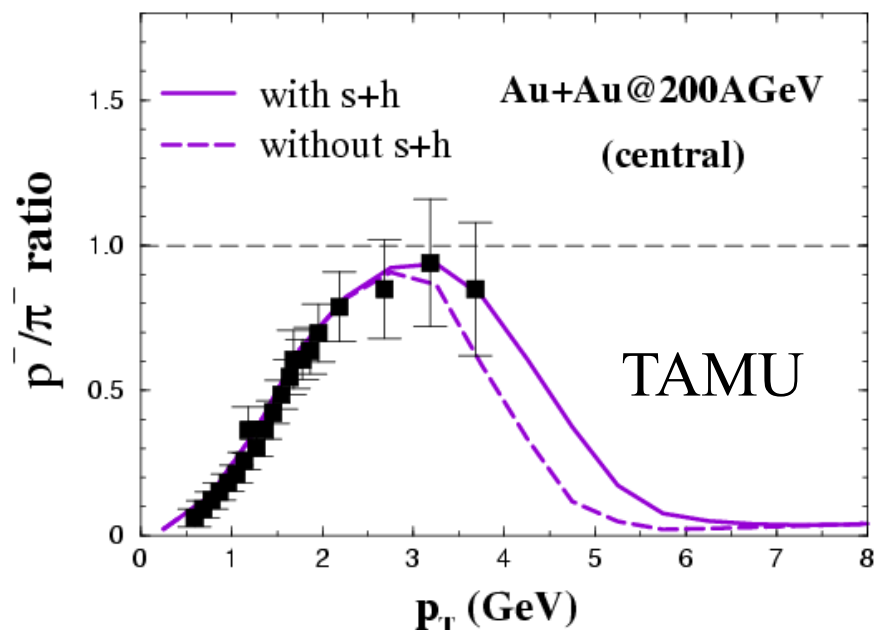
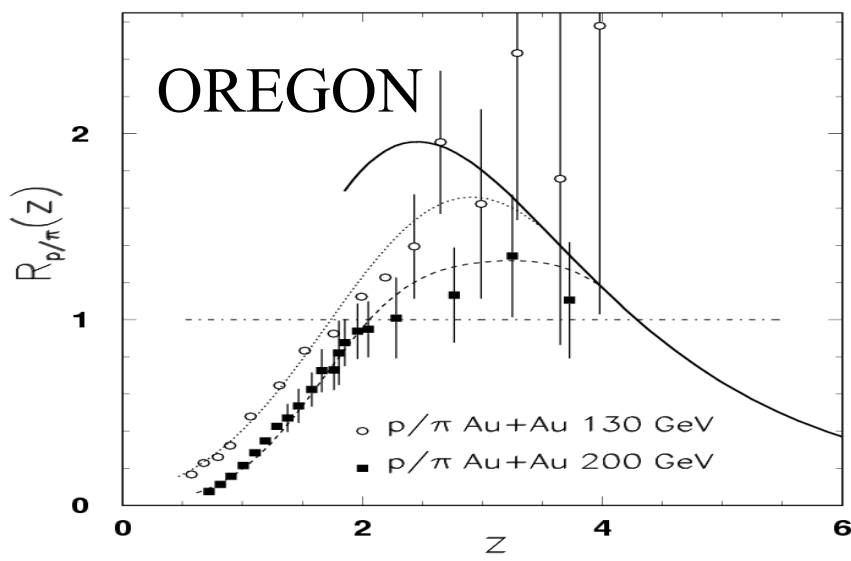
Mattiello, Sorge, Stocker, and Greiner, PRC 55, 1443 (1997)



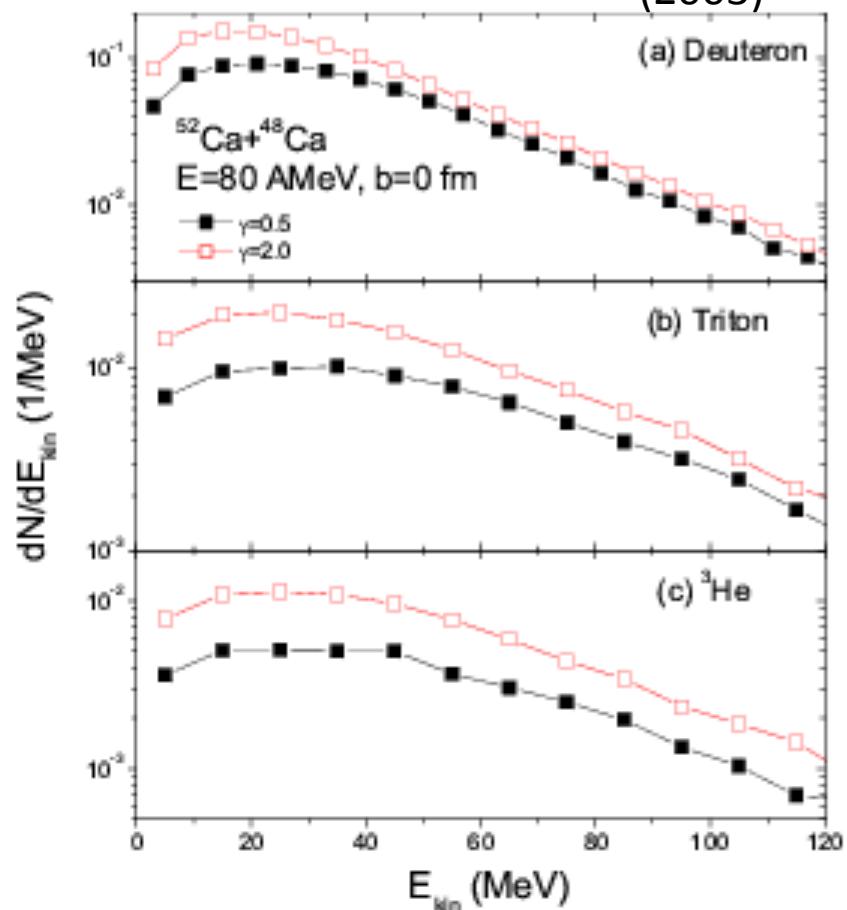
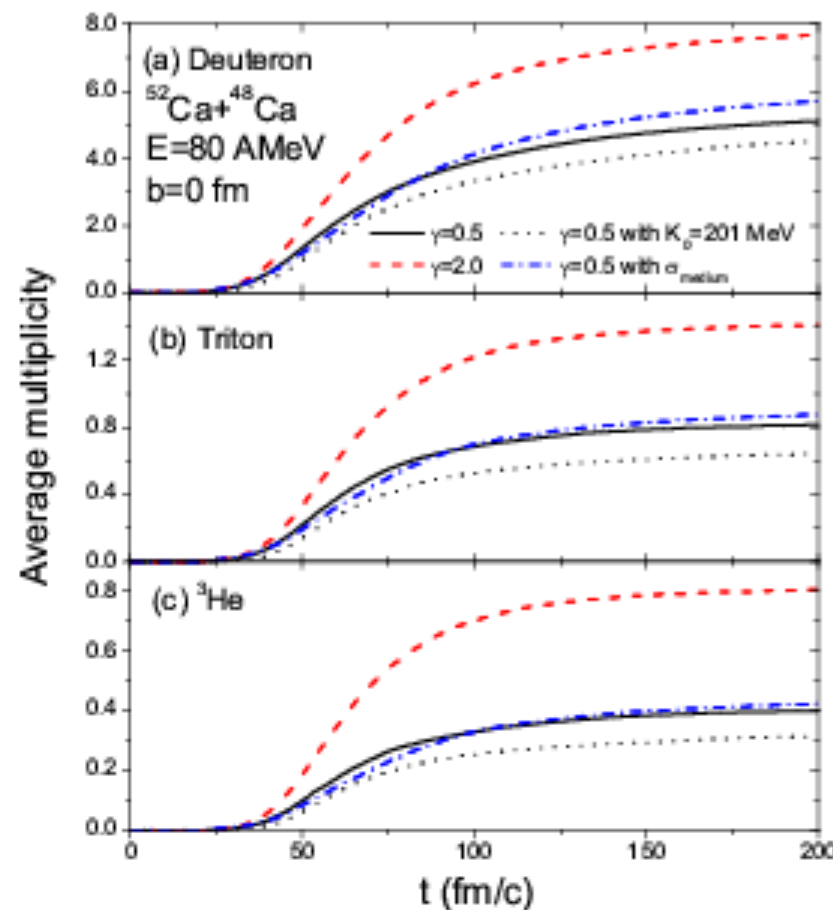
- 2000s
 - 1) Hwa and Yang, PRC 67, 034902 (2003): Standard Wigner calculation using fitted thermal and shower partons.
 - 2) Greco, Ko , and Levai, PRL 90, 202301 (2003): Standard Wigner calculation using thermal and jet partons.
 - 3) Fries, Meuller, Nonaka, and Bass, PRL 90, 202303 (2003): Standard Wigner calculation using thermal partons.
 - 4) Chen, Ko, and Li, NPA 729, 809 (2003): Standard Wigner calculation using IBUU transport model; cluster-cluster HBT.
 - 5) Greco, Ko, and Rapp, PLB 595, 202 (2004): Standard Wigner calculation for charmonia production.
 - 6) Chen, Greco, Ko, Lee, and Liu, PLB 601, 34 (2004): Standard Wigner calculation for pentaquark baryon production.
 - 7) Kanada-En' yo and Meuller, PRC 74, 061901(R) (2006): Effect of p-wave coalescence for $\Lambda(1520)$ production in HIC.
 - 8) Chen, Ko, Liu, and Nielsen, PRC 76, 014906 (2007): Standard Wigner calculation for $D_{sJ}(2317)$ production in HIC.
 - 9) Oh, Lin, and Ko, PRC 80, 064902 (2009): Transport approach with $n+p \rightarrow \pi+d$ vs standard Wigner calculation.

Large proton to pion ratio

Quark coalescence or recombination can explain observed large p/pi ratio at intermediate transverse momenta in central Au+Au collisions.



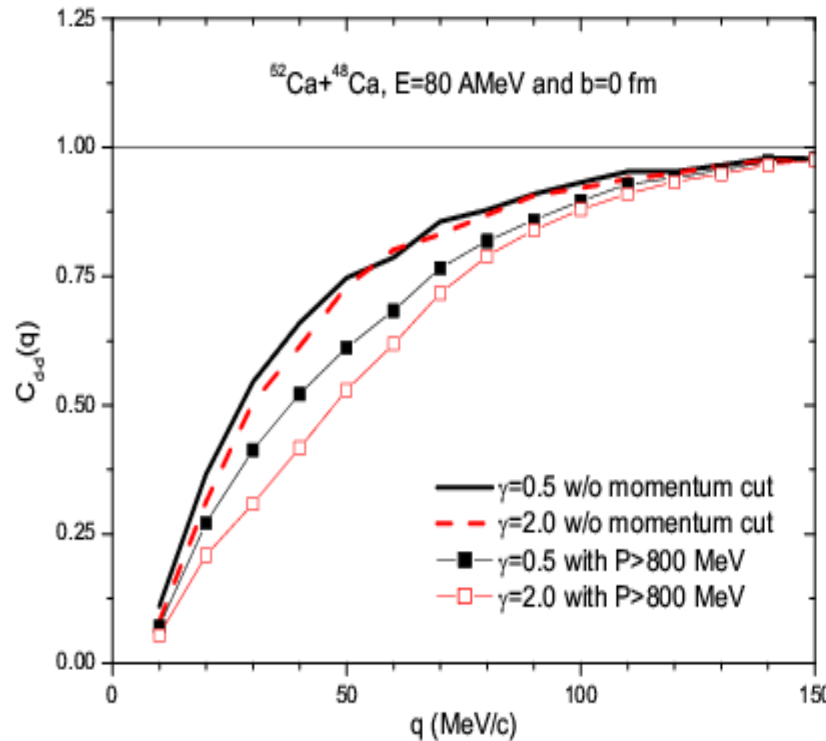
Light clusters from collisions of asymmetric nuclei



- Symmetry energy effects are about 51%, 73%, and 100% on deuteron, triton and He yields with stiffer one ($\gamma=2.0$) producing more
- Symmetry energy effects stronger on lower energy light clusters
- Effects of isoscalar energy and NN cross sections small

Two-deuteron correlation functions Chen et al., NPA 729, 809 (2003)

$$C(\mathbf{P}, \mathbf{q}) = \frac{\int d^4x_1 d^4x_2 g(\mathbf{P}/2, x_1) g(\mathbf{P}/2, x_2) |\phi(\mathbf{q}, \mathbf{r})|^2}{\int d^4x_1 g(\mathbf{P}/2, x_1) \int d^4x_2 g(\mathbf{P}/2, x_2)}$$



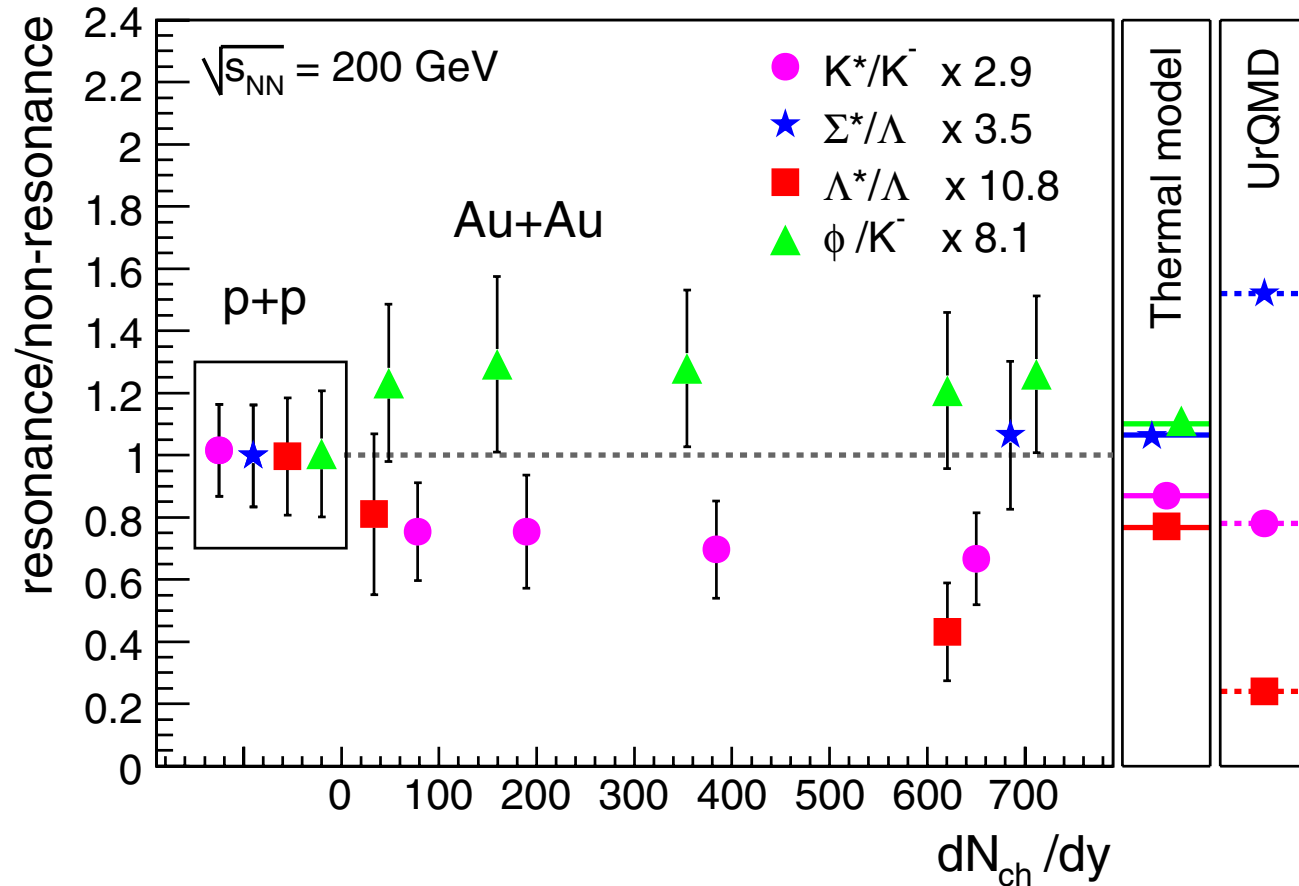
$$\begin{aligned} x_i &= (\mathbf{r}_i, t_i) \\ \mathbf{P} &= \mathbf{p}_1 + \mathbf{p}_2, \quad \mathbf{q} = \frac{\mathbf{p}_1 - \mathbf{p}_2}{2} \\ \mathbf{r} &= \mathbf{r}_1 - \mathbf{r}_2 \\ &+ \frac{1}{2}(\mathbf{r}_1 + \mathbf{r}_2)(\mathbf{v}_1 - \mathbf{v}_2) \end{aligned}$$

Include final-state repulsive nuclear s-wave and Coulomb interactions

Anticorrelations of pairs of high total momentum are affected by symmetry energy with stiffer one giving a larger strength, about 20% at $q=40$ MeV/c.

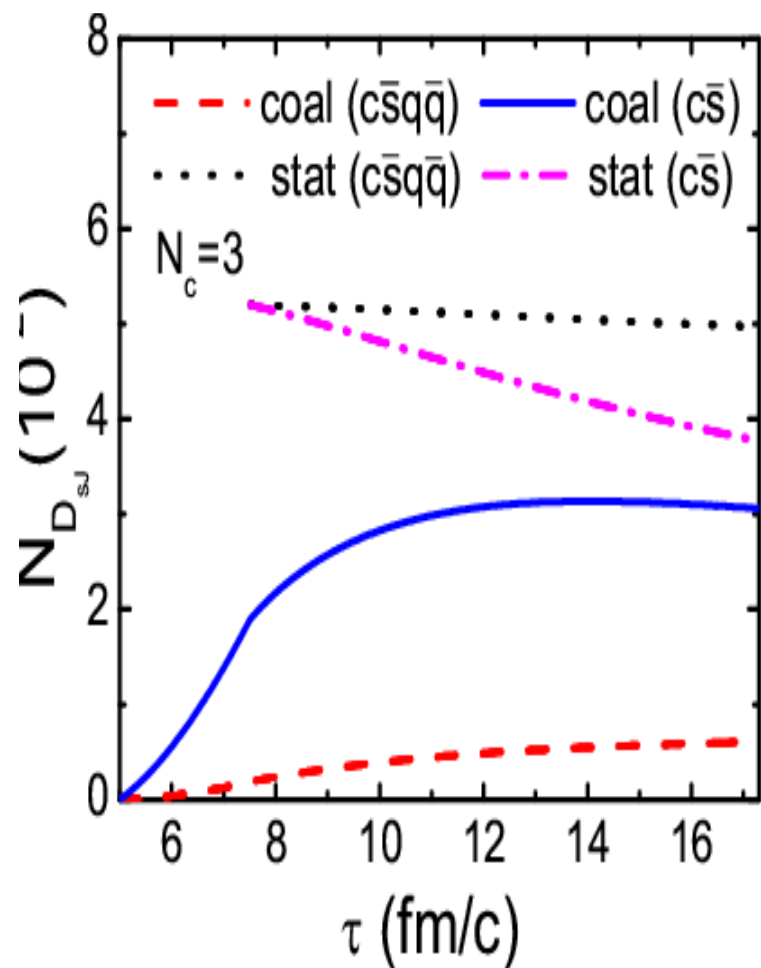
Suppression of $\Lambda(1520)$ in HIC

Abelev [Star Collaboration],
PRL 97, 132301 (2006)

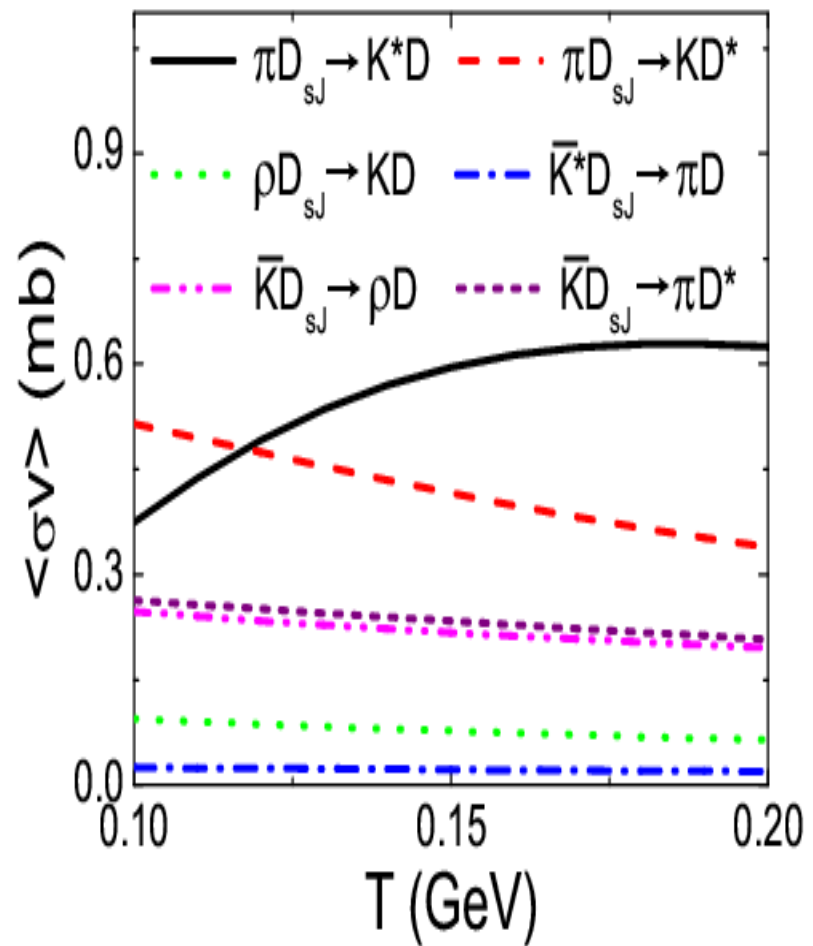


- Measured $\Lambda(1520)/\Lambda(1115)$ ratio is significantly smaller than thermal model prediction, but can be explained by the coalescence model after taking into account the p-wave state of strang quark in $\Lambda(1520)$ (Kanada-En'yo and Meuller, PRC 74, 061901(R) (2006)).

D_{sJ} production at RHIC



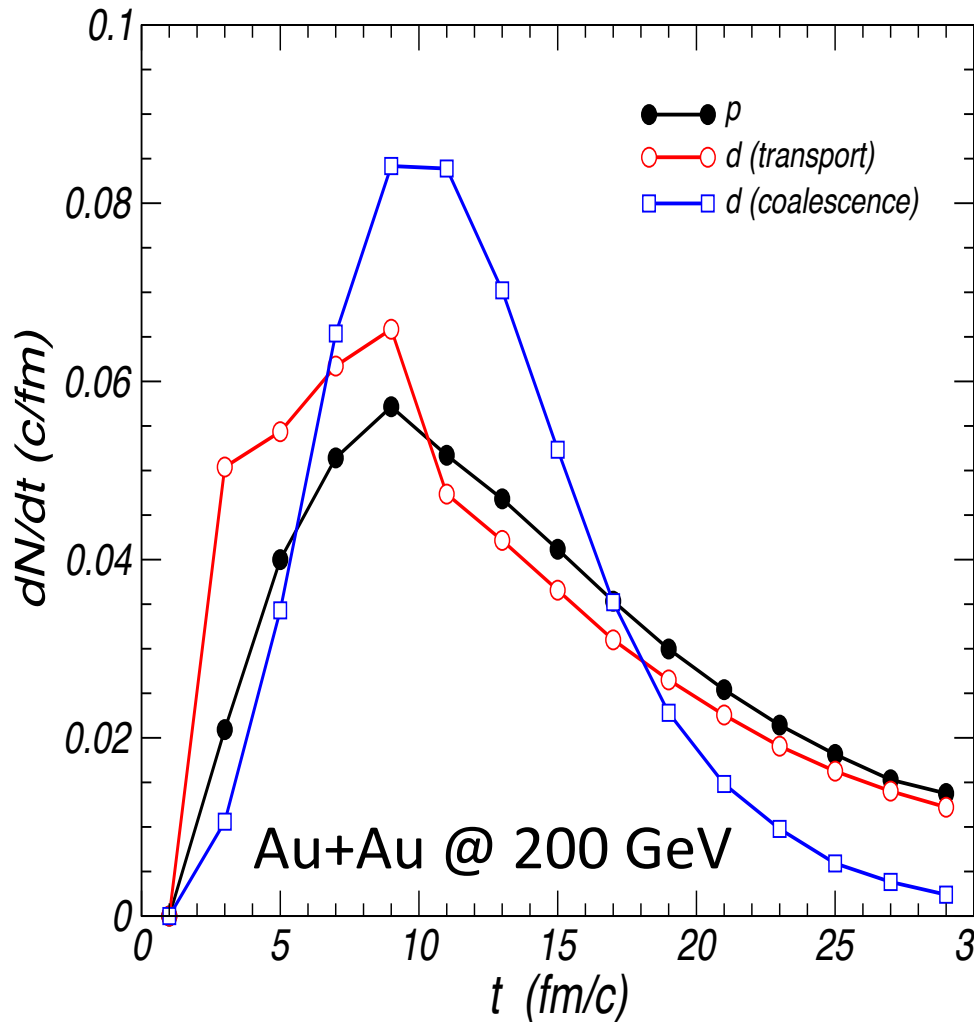
Chen, Liu, Nielsen & Ko, PRC 76, 064903 (2007))



- Cross sections are for four-quark state and larger by ~ 9 for two-quark state.
- Final yield is sensitive to the quark structure of D_{sJ}

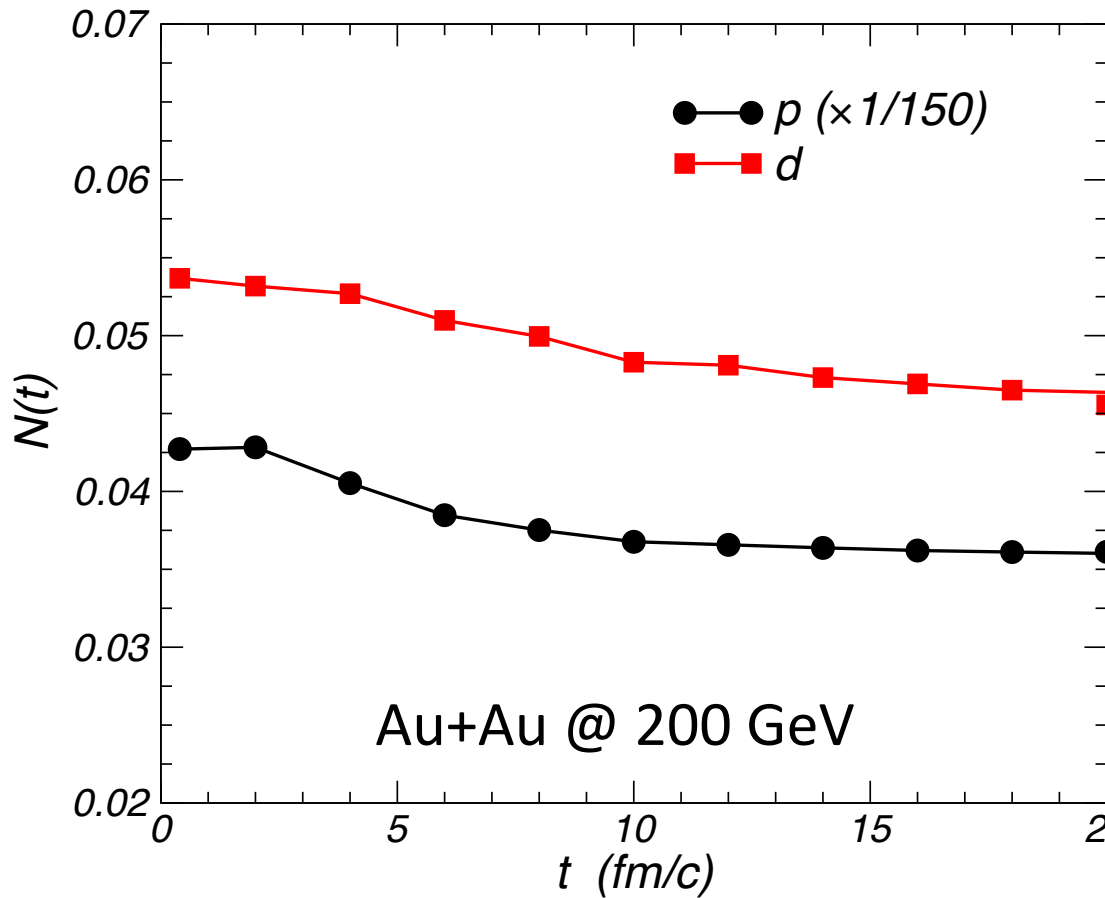
Deuteron emission time distributions

Oh, Lin & Ko, PRC 80,
064902 (2009)



- Based on a relativistic transport model (ART) by adding $NN \leftrightarrow \pi d$ with empirical cross sections.
- Similar emission time distributions for protons and deuterons in coalescence model
- Slight different deuteron early emission time distribution in transport and coalescence models

Time evolution of proton and deuteron numbers



- Both proton and deuteron numbers decrease only slightly with time → early chemical equilibration?

- 2010s
 - 1) Zhang et al, PLB 684, 224 (2010): Standard Wigner calculation using AMPT for hypernuclei production in HIC.
 - 2) Cho et al. [Exhic Collaboration], PRL 106, 212001 (2011); PRC 84, 064910 (2011): Exotic hadrons production.
 - 3) G. Chen et al., PRC 86, 054910 (2012): Simplified coalescence based on dr and dp considerations using PACIAE for antimatter production in HIC.
 - 4) Cho, PRC 91, 054914 (2015): d-wave coalescence for $\psi(2S)$ using both Gaussian and Coulomb wave functions.
 - 5) Sun and Chen, PLB 751, 272 (2015): Antimatter production in HIC based on standard Wigner calculation using blast wave model.
 - 6) Zhu, Ko, and Yin, PRC 92, 064911 (2015): Light nuclei from standard Wigner calculation using AMPT.

.....

Exotic hadron yields at RHIC and LHC

TABLE V. Exotic hadron yields in central Au + Au collisions at $\sqrt{s_{NN}} = 200$ GeV at RHIC and in central Pb + Pb collisions at $\sqrt{s_{NN}} = 5.5$ TeV at LHC from the quark coalescence ($2q/3q/6q$ and $4q/5q/8q$) and the hadron coalescence (Mol.), as well as from the statistical model (Stat.)

	RHIC				LHC			
	$2q/3q/6q$	$4q/5q/8q$	Mol.	Stat.	$2q/3q/6q$	$4q/5q/8q$	Mol.	Stat.
Mesons								
$f_0(980)$	3.8, 0.73($s\bar{s}$)	0.10	13	5.6	10, 2.0 ($s\bar{s}$)	0.28	36	15
$a_0(980)$	11	0.31	40	17	31	0.83	1.1×10^2	46
$K(1460)$	—	0.59	3.6	1.3	—	1.6	9.3	3.2
$D_s(2317)$	1.3×10^{-2}	2.1×10^{-3}	1.6×10^{-2}	5.6×10^{-2}	8.7×10^{-2}	1.4×10^{-2}	0.10	0.35
T_{cc}^1 ^a	—	4.0×10^{-5}	2.4×10^{-5}	4.3×10^{-4}	—	6.6×10^{-4}	4.1×10^{-4}	7.1×10^{-3}
$X(3872)$	1.0×10^{-4}	4.0×10^{-5}	7.8×10^{-4}	2.9×10^{-4}	1.7×10^{-3}	6.6×10^{-4}	1.3×10^{-2}	4.7×10^{-3}
$Z^+(4430)$ ^b	—	1.3×10^{-5}	2.0×10^{-5}	1.4×10^{-5}	—	2.1×10^{-4}	3.4×10^{-4}	2.4×10^{-4}
T_{cb}^0 ^a	—	6.1×10^{-8}	1.8×10^{-7}	6.9×10^{-7}	—	6.1×10^{-6}	1.9×10^{-5}	6.8×10^{-5}
Baryons								
$\Lambda(1405)$	0.81	0.11	1.8–8.3	1.7	2.2	0.29	4.7–21	4.2
Θ^+ ^b	—	2.9×10^{-2}	—	1.0	—	7.8×10^{-2}	—	2.3
$\bar{K}KN$ ^a	—	1.9×10^{-2}	1.7	0.28	—	5.2×10^{-2}	4.2	0.67
$\bar{D}N$ ^a	—	2.9×10^{-3}	4.6×10^{-2}	1.0×10^{-2}	—	2.0×10^{-2}	0.28	6.1×10^{-2}
\bar{D}^*N ^a	—	7.1×10^{-4}	4.5×10^{-2}	1.0×10^{-2}	—	4.7×10^{-3}	0.27	6.2×10^{-2}
Θ_{cs} ^a	—	5.9×10^{-4}	—	7.2×10^{-3}	—	3.9×10^{-3}	—	4.5×10^{-2}
BN ^a	—	1.9×10^{-5}	8.0×10^{-5}	3.9×10^{-5}	—	7.7×10^{-4}	2.8×10^{-3}	1.4×10^{-3}
B^*N ^a	—	5.3×10^{-6}	1.2×10^{-4}	6.6×10^{-5}	—	2.1×10^{-4}	4.4×10^{-3}	2.4×10^{-3}
Dibaryons								
H ^a	3.0×10^{-3}	—	1.6×10^{-2}	1.3×10^{-2}	8.2×10^{-3}	—	3.8×10^{-2}	3.2×10^{-2}
$\bar{K}NN$ ^b	5.0×10^{-3}	5.1×10^{-4}	0.011–0.24	1.6×10^{-2}	1.3×10^{-2}	1.4×10^{-3}	0.026–0.54	3.7×10^{-2}
$\Omega\Omega$ ^a	3.2×10^{-5}	—	1.5×10^{-5}	6.4×10^{-5}	8.6×10^{-5}	—	4.4×10^{-5}	1.9×10^{-4}
H_c^{++} ^a	3.0×10^{-4}	—	3.3×10^{-4}	7.5×10^{-4}	2.0×10^{-3}	—	1.9×10^{-3}	4.2×10^{-3}
$\bar{D}NN$ ^a	—	2.9×10^{-5}	1.8×10^{-3}	7.9×10^{-5}	—	2.0×10^{-4}	9.8×10^{-3}	4.2×10^{-4}
BNN ^a	—	2.3×10^{-7}	1.2×10^{-6}	2.4×10^{-7}	—	9.2×10^{-6}	3.7×10^{-5}	7.6×10^{-6}

^aParticles that are newly predicted by theoretical model.

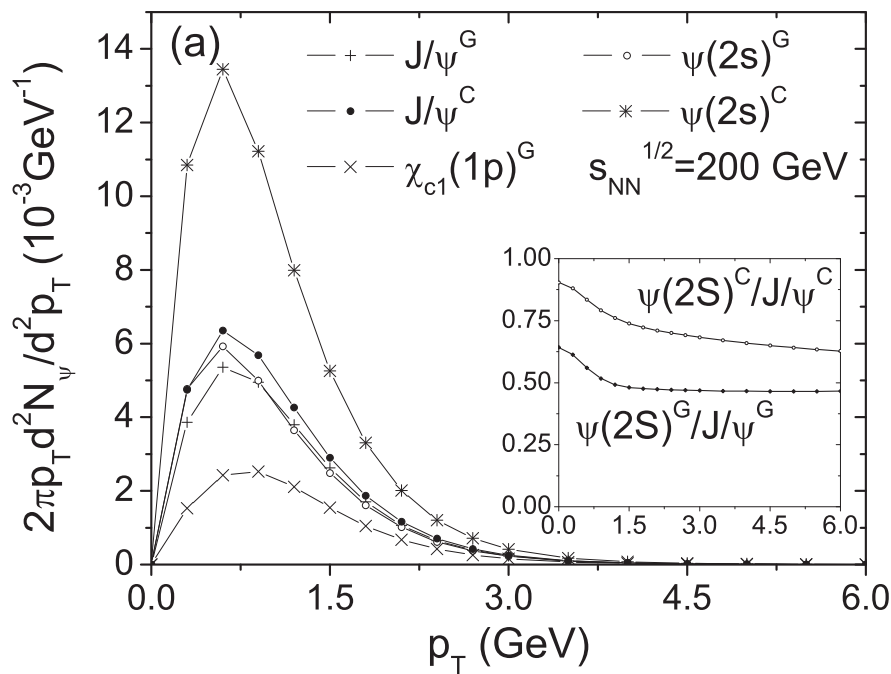
^bParticles that are not yet established.

■ Most yields are sufficient large ($>10^{-5}$) 22

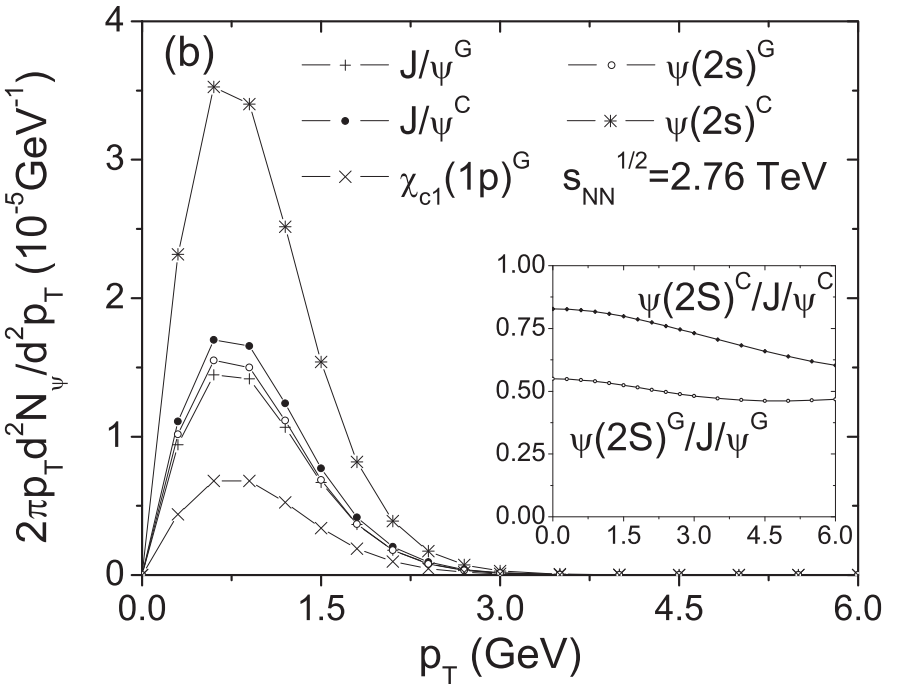
Wave function effects on charmonia production

Cho, PRC 91, 054914 (2015)

Au+Au @ 200 GeV

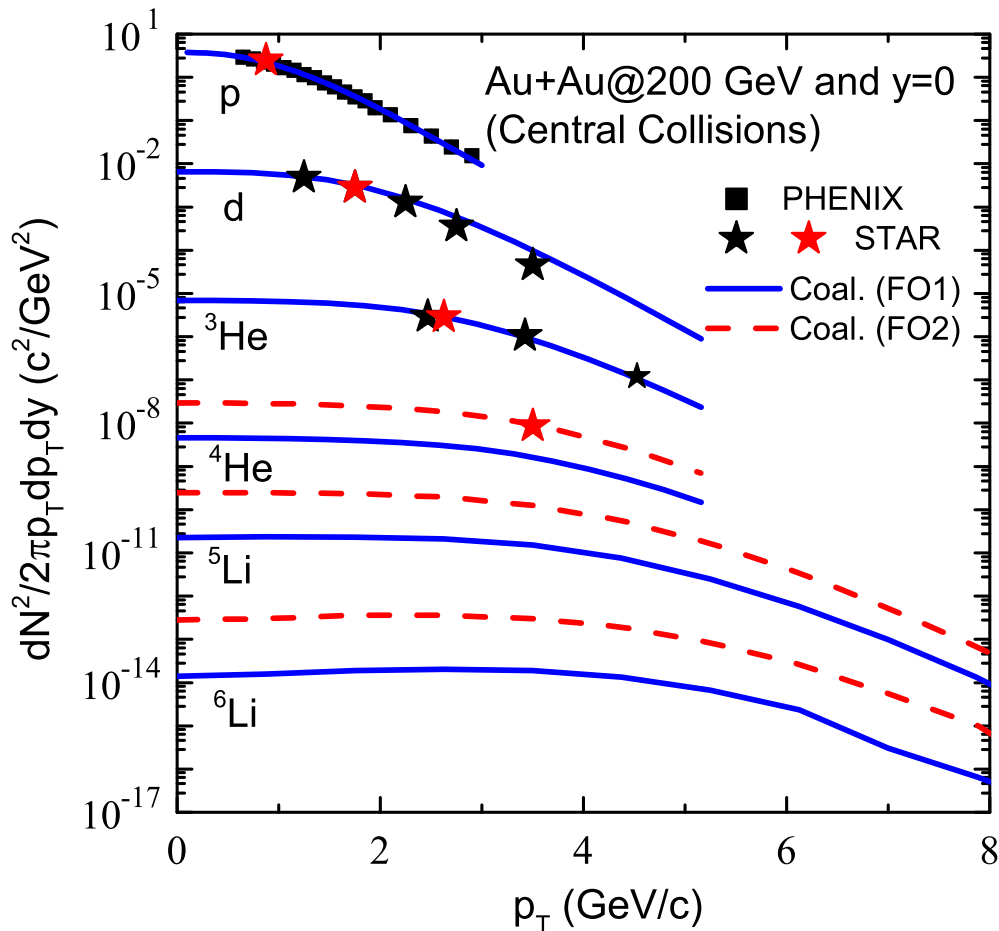


Pb+Pb @ 2.76 TeV



- Coulomb wave function gives larger production than the Gaussian wave function.
- Nuclear modification factor ratio between $\psi(2S)$ and J/ψ is sensitive to their wave functions and thus can serve as a probe.

Binding energy effect on antimatter production



Sun and Chen, PLB 751,
272 (2015)

- 4He is formed earlier because its larger binding energy.
- Assuming a similar effect for ${}^5\text{Li}$ and ${}^6\text{Li}$ leads to their enhanced production.

Table 1

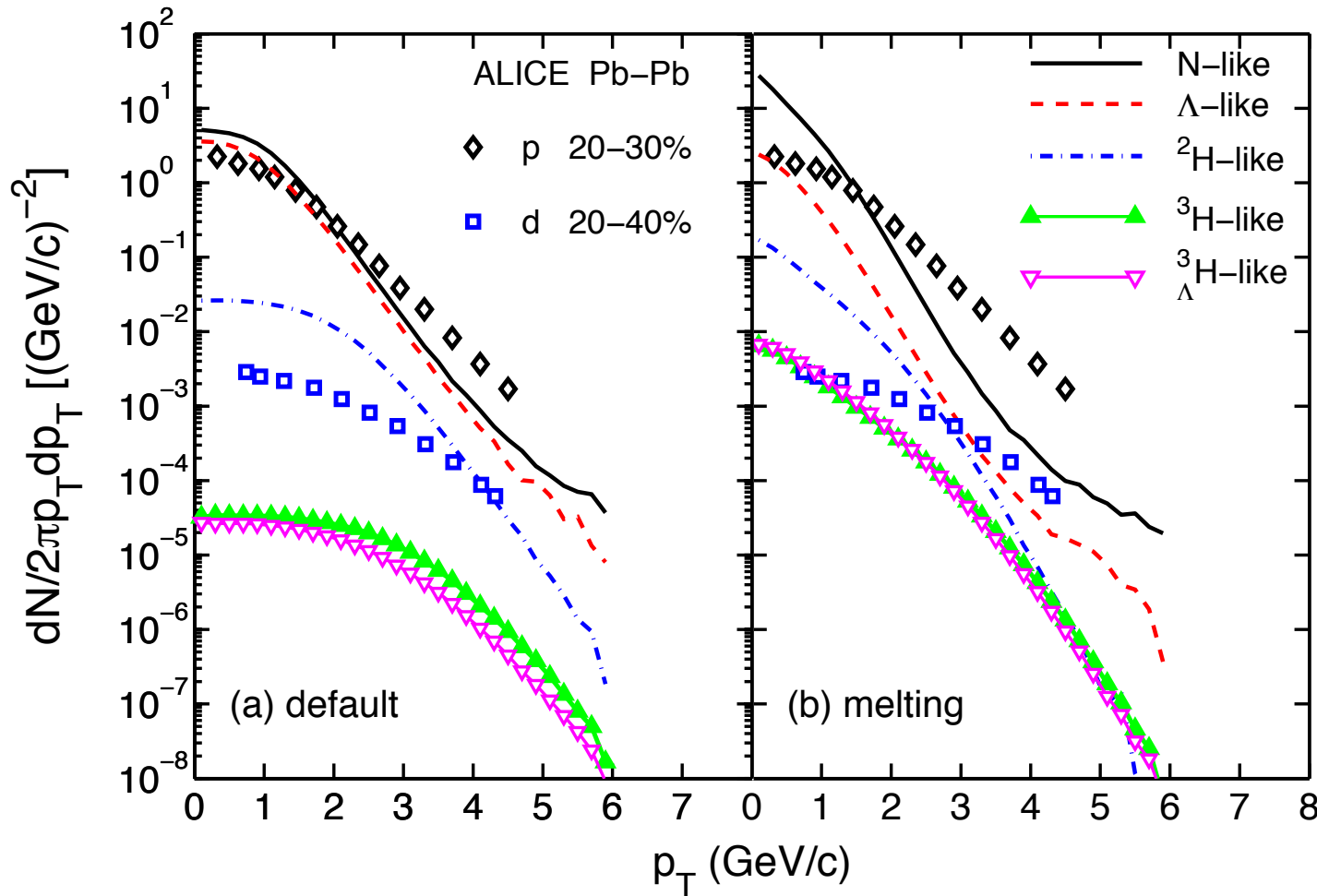
Parameters of the blast-wave-like analytical parametrization for (anti-)nucleon phase-space freezeout configuration.

	T (MeV)	ρ_0	R_0 (fm)	τ_0 (fm/c)	$\Delta\tau$ (fm/c)	ξ_p	$\xi_{\bar{p}}$
FO1	111.6	0.98	15.6	10.55	3.5	10.45	7.84
FO2	111.6	0.98	12.3	8.3	3.5	21.4	16.04

Pb+Pb @ 2.76 GeV from AMPT

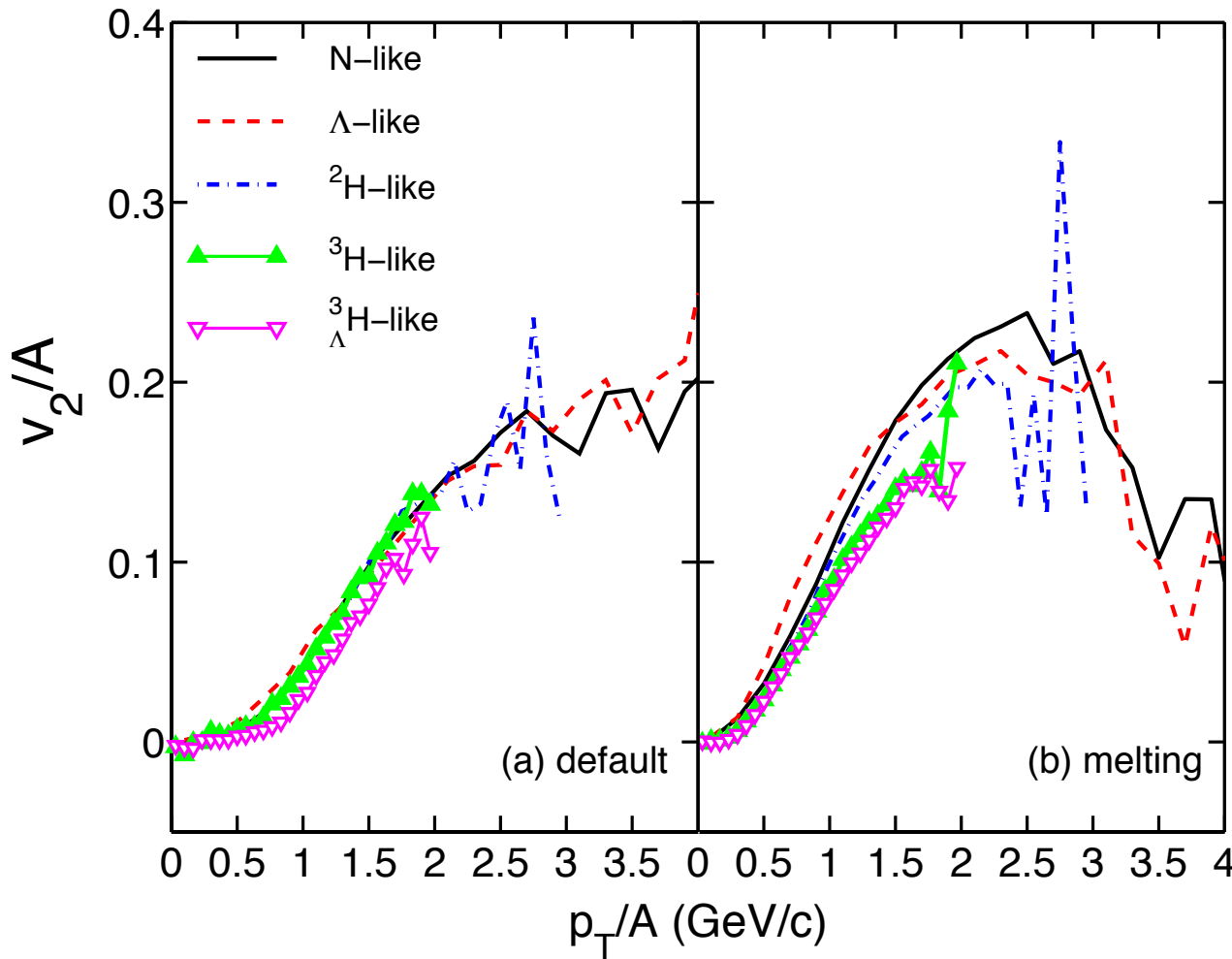
Transverse momentum spectra

Zhu, Ko & Yin, PRC
92, 064911 (2015)



- Default AMPT works better than string melting due to baryon problem in latter, but both not perfect.

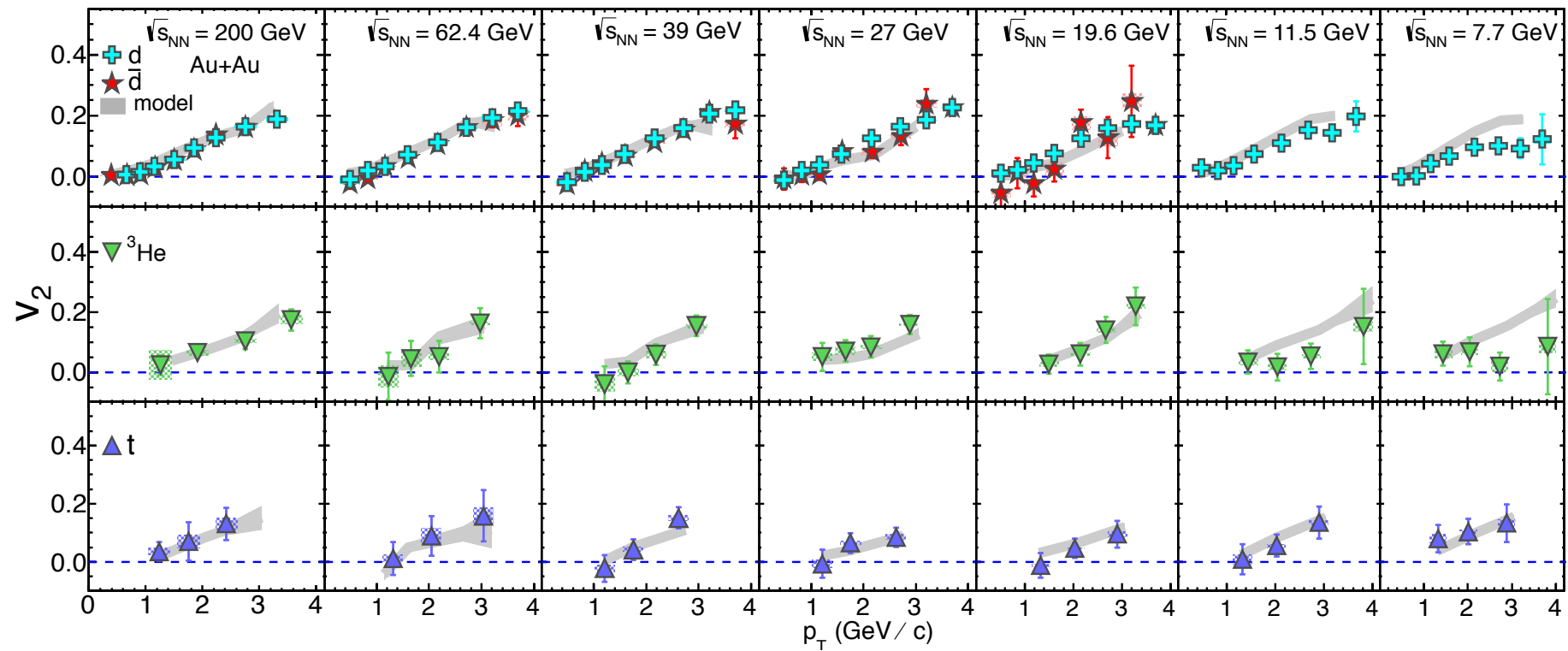
Nucleon number scaled elliptic flows



- Approximate nucleon number scaling is predicted, particularly in default AMPT. Of interest to compare with future experiments.

Elliptic flow from STAR Beam Energy Scan

arXiv:1601.0705



AMPT +Coalescence reproduces data reasonably well

In quantum Wigner approach, wave functions of particles 1 and 2 are Gaussian wave packets

$$\begin{aligned}\phi_i(x'_i - x_i) &= \frac{1}{(\pi\delta^2)^{1/4}} \exp\left[-\frac{(x'_i - x_i)^2}{2\delta^2}\right] \exp(ik_i x'_i) \\ W(x'_i, k'_i) &= 2e^{-(x'_i - x_i)^2/\delta^2} e^{-\delta^2(k'_i - k_i)^2}\end{aligned}$$

Using harmonic oscillator wave functions for the wave function of formed particle 3

$$\begin{aligned}\Phi_n(x) &= \left(\frac{m\omega}{\pi\hbar}\right)^{1/4} \frac{1}{\sqrt{2^n n!}} H_n(\xi) e^{-\xi^2/2} \\ \xi &= \sqrt{\frac{m\omega}{\hbar}} x, \quad H_n(\xi) : \text{Hermite polynomials}\end{aligned}$$

leads to recurrence relations for the overlap integrals of Wigner functions

$$\begin{aligned}
\overline{W}_{n+5} &= -\frac{1}{\Lambda_5}(\Lambda_4 \overline{W}_{n+4} + \Lambda_3 \overline{W}_{n+3} + \Lambda_2 \overline{W}_{n+2} + \Lambda_1 \overline{W}_{n+1} + \Lambda_0 \overline{W}_n) \\
\Lambda_0 &= -[(1+\alpha)^2 + n](1-\alpha)^2, \\
\Lambda_1 &= [\alpha(1-\alpha) + 2(x/\sigma)^2 + 2\alpha^2(k\sigma)^2 + n + 1](1-\alpha)^2 x \\
\Lambda_2 &= [(1-\alpha)(\alpha^2 + 4\alpha + 1) - 2(x/\sigma)^2(3\alpha + 1) - 2\alpha(k\sigma)^2(-\alpha^2 + 3\alpha + 2) \\
&\quad - 2(n+2)(1+\alpha)^2(1-\alpha)](1-\alpha), \\
\Lambda_3 &= [\alpha(1-\alpha)^2 + 2(x/\sigma)^2(3\alpha^2 - 2\alpha - 1) + 2\alpha(k\sigma)^2(\alpha^3 - 3\alpha^2 + 9\alpha - 7) \\
&\quad - 2(n+3)(1+\alpha)^2(1-\alpha)], \\
\Lambda_4 &= [2(x/\sigma)^2 + 2\alpha^2(k\sigma)^2 - (n+4)(1-\alpha)^2](1+\alpha)^2, \\
\Lambda_5 &= -(n+5)(1+\alpha)^2, \quad \alpha = 2\delta^2/\sigma^2, \quad \sigma = \sqrt{\frac{\hbar}{m\omega}}
\end{aligned}$$

In the special case of $\alpha=1$

$$\begin{aligned}
\overline{W}_{n+1} &= \frac{v}{n+1} \overline{W}_n, \quad v = \frac{1}{2} \left(\frac{x^2}{\sigma^2} + k^2 \sigma^2 \right) \\
\overline{W}_0 &= \exp(-v), \quad \overline{W}_n = \frac{v^n}{n!} e^{-v}
\end{aligned}$$

In 3-dimensions, the overlap integral of Wigner function is

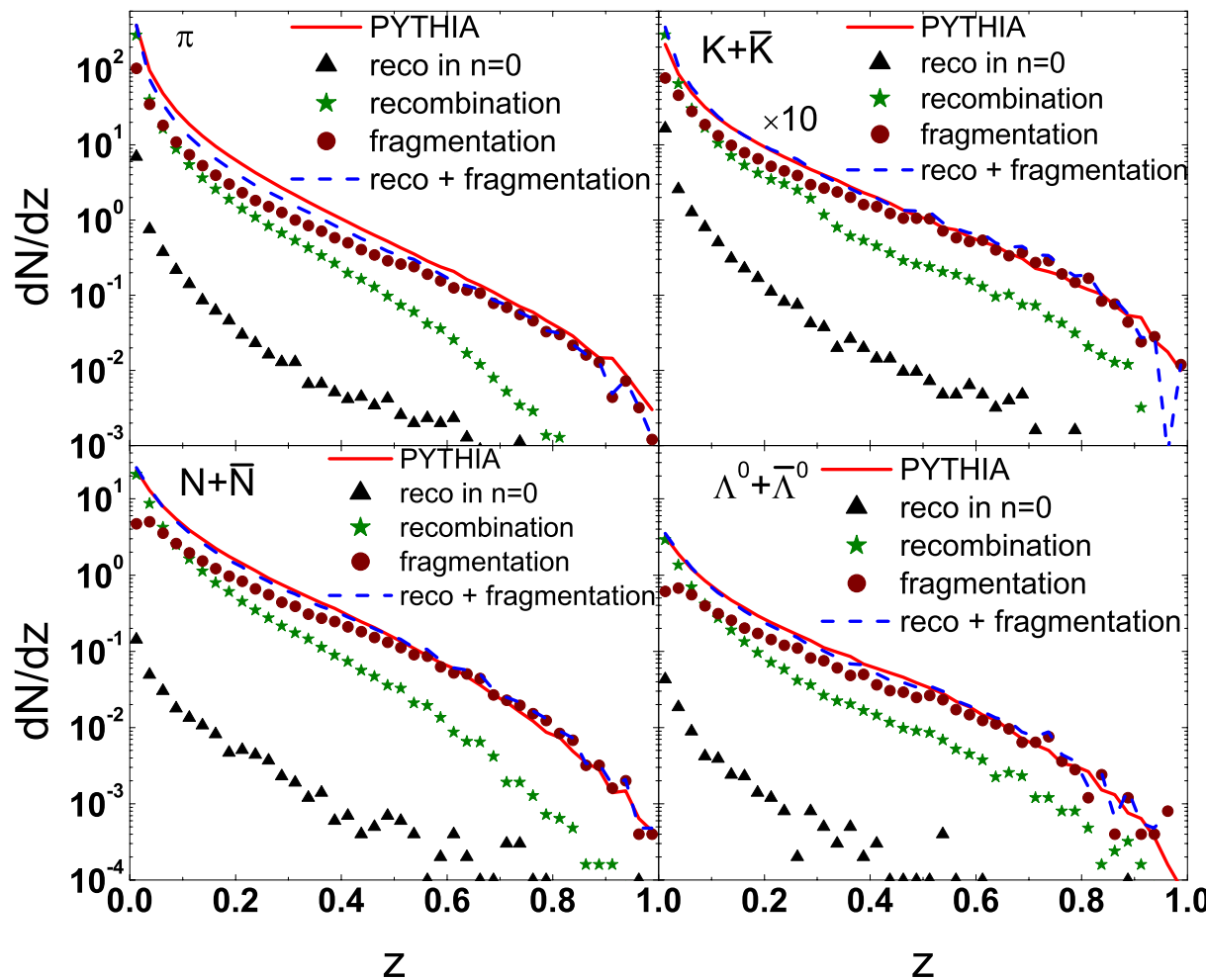
$$\begin{aligned}
\overline{W}_n(\mathbf{x}, \mathbf{k}) &= \sum_{n_x+n_y+n_z=n} \overline{W}_{n_x}(x, k_x) \overline{W}_{n_y}(y, k_y) \overline{W}_{n_z}(z, k_z) \\
&= \sum_{n_x+n_y+n_z=n} \frac{v_x^{n_x}}{n_x!} e^{-v_x} \cdot \frac{v_y^{n_y}}{n_y!} e^{-v_y} \cdot \frac{v_z^{n_z}}{n_z!} e^{-v_z} \\
&= \frac{1}{n!} e^{-v} \sum_{n_x+n_y+n_z=n} \frac{n!}{n_x! n_y! n_z!} v_x^{n_x} v_y^{n_y} v_z^{n_z} \\
&= \frac{v^n}{n!} e^{-v} \\
v &= v_x + v_y + v_z = \frac{1}{2} \left(\frac{\mathbf{x}^2}{\sigma^2} + \mathbf{k}^2 \sigma^2 \right)
\end{aligned}$$

Jet fragmentation via shower partons recombination

Han, Fries @ Ko, arXiv:1601:00768

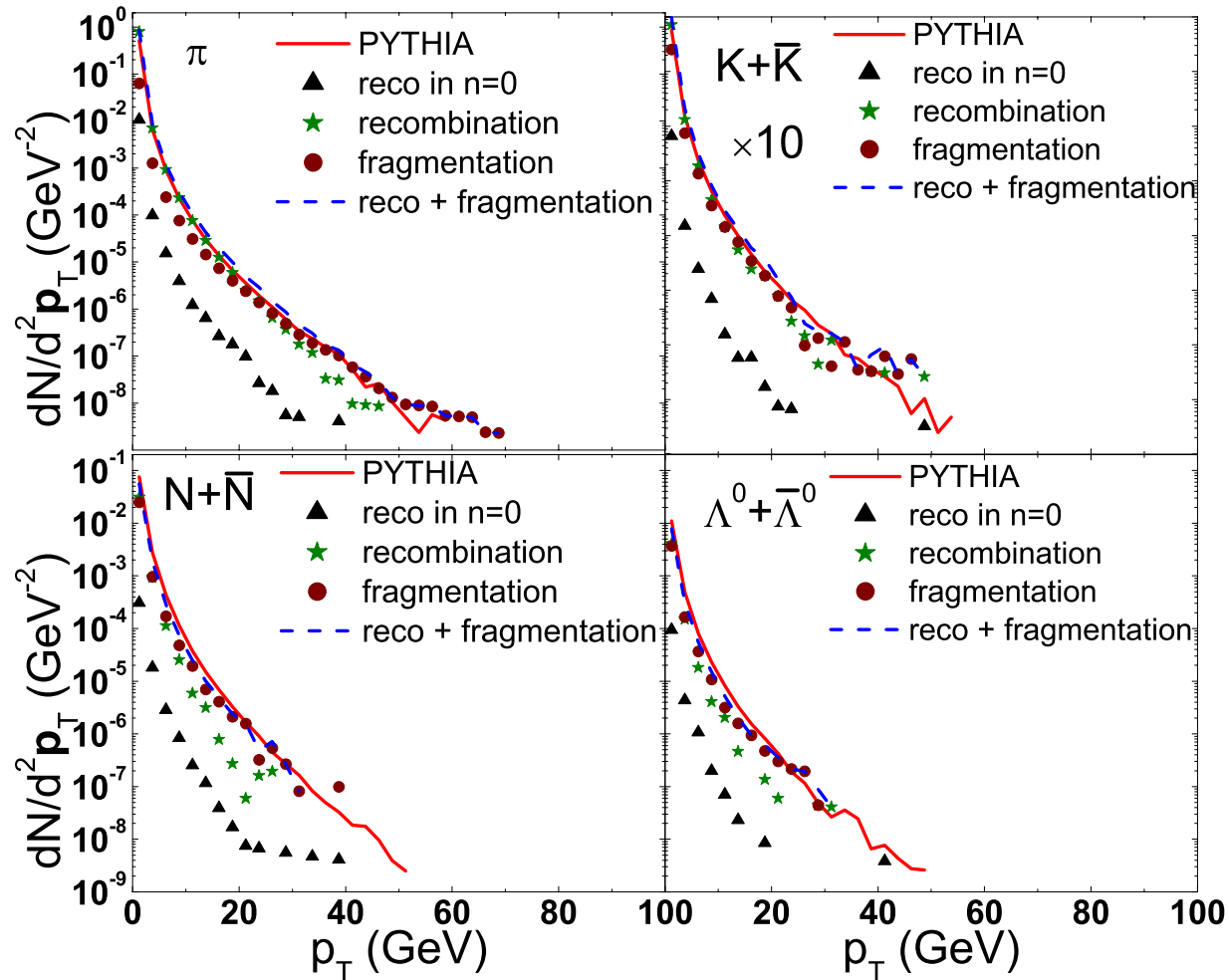
- Using PYTHIA to obtain momenta of shower partons from jets produced in e^+e^- @ 200 GeV.
- Spatial information of shower partons are determined by taking their lifetimes to be inverse of their virtualities and propagating accordingly.
- Final gluons with low virtualities are decayed to quark-antiquark pairs.
- Using quantum Wigner calculation to coalescence shower partons to hadrons in an event by event basis up to hadron excited states with $n=8$ harmonic oscillator wave functions.
- Remnant shower partons not used in coalescence are formed into short strings and converted to hadrons by string fragmentation.
- Results are compared with those from PYTHIA via fragmentation of the entire string.

Longitudinal momentum fraction spectra



- Recombination contribution is dominated by excited states.
- Contribution from remnant short strings dominates at large z .

Transverse momentum spectra



- Recombination contribution is dominated by excited states.
- Contribution from remnant short strings dominates at large z .

Summary

- The coalescence model has a long history. It was introduced as a phenomenological model to understand deuteron production in reactions induced by energetic protons on nuclei.
- It is now understood in terms of the sudden approximation and is thus applicable if cluster production is fast compared to the time over which the system changes appreciably and seems to be supported by study based on the kinetic or transport approach.
- It has been used for describing not only light clusters production from hadronic matter but also hadron production from QGP in heavy ion collisions, even from jets.
- It provides a means to probe the properties of clusters as well as hadrons as their yields in the coalescence model depend on their internal structures.
- It remains a challenge to understand the relation between the coalescence model and the statistical model for particle production.